International Journal of Progressive Sciences and Technologies (IJPSAT)
ISSN: 2509-0119.

http://ijpsat.ijsht-journals.org
Vol. 23 No. 2 November 2020, pp. 541-554

# *Insights into the Chemical Bonding in Microhydrated Protons from Molecular Orbital and Population Analysis Methods*

Anant Babu Marahatta[1, 2]

[1]Department of Chemistry, Amrit Science Campus, Tribhuvan University, Kathmandu, Nepal
[2]Chemistry Subject Committee, Kathford International College of Engineering and Management (Affiliated to Tribhuvan University), Kathmandu, Nepal



**Abstract – Research works related to investigate molecular electronic structures and thermodynamic stabilities simply by looking into the position of concerned atomic nuclei in the theoretically optimized molecular geometries do not give quantitative picture of the chemical bonding in respect to electron density distributions around atoms and bonds between the atoms. Therefore, total molecular electron density surfaces, and molecular orbitals (MOs) iso-surfaces & contours must be analyzed deeply while interpreting chemical bonds and electronic interactions quantum mechanically. In this paper, how these electron density surfaces (EDSs) actually provide meaningful explanation to the orbital interactions and atomic bonding in microhydrated protons: Hydronium ($H_3O^+$), Zundel ($H_5O_2^+$), and Eigen ($H_9O_4^+$), and their overviews are reported briefly. The MOs and Mulliken population analysis methods are used to extract their chemical bond related information from their own DFT derived molecular wavefunctions (Ψ), and then all the EDSs are examined thoroughly. The MOs analysis reveals that the total molecular electron density surface of each cation defines a closed 3D structural entity plus an exact distribution of electron cloud around the specific bonds, the iso-surface of each MO displays a delocalized type electron density properly along with approximating a region in which bonding electrons are likely to be found and confirming orbital type interactions in atomic bonding, and the contour lines of all the MOs measure the electron amplitudes quantitatively. Additionally, the Mulliken derived partial atomic charge value on each atom of them quantify and compare specific bonding interactions numerically.**

**Keywords – Hydrated protons, Molecular wavefunctions, Contour maps, and Chemical bond analysis.**

## I. INTRODUCTION

After realizing the fundamental assumptions of empirically proposed Grotthuss mechanism in understanding proton dynamics, and observing the involvement of three most stable hydrated states of protons: Hydronium ($H_3O^+$), Zundel ($H_5O_2^+$), and Eigen ($H_9O_4^+$) in proton transport and proton-hopping processes, intense theoretical studies have been carried out concentrating on their electronic structures, chemical energetics, thermodynamic stabilities, HOMO−LUMO interactions, electronic polarizabilities etc. along with their critical roles in proton diffusion mechanism in several aqueous type media [1], [2], [3], [4], [5]. Beside this, the ubiquity of aqueous proton dynamics in: (a) acidic aqueous solutions of strong and weak electrolytes, (b) several types of proton exchange semipermeable membranes while incorporating into the membrane electrode assembly, (c) all the pH-related chemical, biological, industrial, environmental, and catalytic aqueous systems, and (d) fuel cells, redox flow battery technologies, electrolysers etc. [6], [7], [8], [9] has made chemists to undertake series of research works related to give theoretical and experimental insights into the electronic interactions and chemical bonding in $H_3O^+$, $H_5O_2^+$, and $H_9O_4^+$ states of the proton. Amid this, the present research work is aimed at analyzing the theoretical calculations performed on these three hydrated protons through the two principal methods, *viz*. (a) Molecular orbitals (hereafter, MOs) analysis and (b) Population analysis, and unveiling the homogeneity of the electron density over them and finding out how it actually provides meaningful

**Corresponding Author:** Anant Babu Marahatta

explanation to the orbital interactions and atomic bonding in them. For this objective, the theoretical calculations carried out on free $H_2O$ molecule are also analyzed by the same methods thoroughly as it is a closely associated molecular component during proton hydration process in the aqueous type solutions.

It is very apparent in proton hydration mechanisms that discrete water molecules around the $H^+$ ion move closer to latter under the influence of their mutual attractive force, and while interacting them to each other, a small change in total electronic energy of these microscopic particles occurs. But, such a small change in total electronic energy is very significant while computing electronic structures of these micro-hydrated protons in the aqueous type solutions, and determining their effective molecular orbitals and electron density surfaces quantitatively [4], [10], [11], [12], [13]. Therefore, an *ab initio* type quantum mechanical model employing hybrid density functional B3LYP method with 6−31G (*d*, *p*) basis set is implemented here as the best alternative computational approach for incorporating such a small change in total electronic energy of the micro-hydrated proton systems $H_3O^+$, $H_5O_2^+$, and $H_9O_4^+$, and optimized their electronic structures in the ground states. By looking at the position of the atomic nuclei (bond distances, and angles) in their theoretically optimized structures, present author has already reported their corresponding structural parameters, ground state molecular geometries, chemical energetics, thermodynamic and kinetic stabilities quantitatively as it is one of the very common practices of theoretical chemists/physicists for estimating as reliable as experimentally observed structural information [4], [5]. However, more quantum mechanical way for interpreting their bonding interactions and structural entities quantitatively is to look seriously at their DFT derived electron densities: direct quantitative pictures for their molecular wavefunctions $\Psi$. As the $\Psi$ can't be seen directly, but can be expressed mathematically as a sum of the products of individual molecular orbitals $\Psi_i$ containing spin paired electrons, we should look at total molecular electron density (a squared of the $\Psi$ ($\Psi^2$)) of each hydrated state seriously and examine how it varies over each ionic specimen through density surface and individual MOs' iso-surfaces and contours mapping techniques carefully [14], [15], [16]. In quantum mechanics, this type of quantitative theoretical inspection is eventually called MOs analysis because the MOs themselves are solutions to the Schrodinger wave mechanical equation, wavefunctions $\Psi$, and electrons' most-probable residing regions [17].

As stated above, the MOs are the electron rich mathematical functions that can be used to depict electronic location and wave like behavior in the molecular specimens. In theoretical calculations, each MO is usually expanded in terms of the atomic orbital (AO) basis functions: Slater-type orbitals (STOs) or Gaussian-type orbitals (GTOs), former represents electron density well in valence region and beyond but difficult to evaluate the integrals while the latter doesn't represent electron density well but easier to evaluate the integrals mathematically [15], [16], [18]. The primary role of these orbitals is to provide us the quantitative information about the contribution of the atoms to each MO. If we are interested to reveal how electronic charges are disseminated in the molecular/ionic systems that are associated with the MOs, AOs, and atomic centers, we must apply the population analysis methods [14]. These methods are mainly based on how the electron density is actually partitioned, and more specifically, if some arbitrary and orbital based scheme is used to partition the molecular wave function, then the method is called Mulliken population analysis [19]. In this study, the same Mulliken method is used for deriving the atomic charges in the $H_2O$ molecule, and $H_3O^+$, $H_5O_2^+$, and $H_9O_4^+$ systems numerically as assigning charges to each atom of them is very significant for getting a rough idea of the charge distribution in the whole ionic specimen that can further quantify and compare specific bonding interactions closely. Even though the Mulliken population analysis is highly basis set dependent: the basis sets which would be best for energy calculations are sometime regarded as worst for population analysis, it is one of the most frequently used analysis methods due to being the most efficient and simplest computational mean for estimating the relative atomic charges of the molecular/ionic specimens. Again, due to its post-processing type computational procedures, it has become a quite popular way to examine the electronic charge redistribution and bond populations in the bulk materials as well as in simple molecular specimens [20].

In theoretical chemistry/physics, both MOs and Mulliken population analysis methods can be routinely carried out by those theoretical models that are developed on the basis of LCAO MO (Linear combination of the atomic orbitals molecular orbitals) approximations [19], [20]. The DFT model is one of them that is based on LCAO-Kohn-Sham ansatz [21], [22]. Several literatures have taken it as an effective theoretical tool to execute these two most common but decent quantum mechanical bonding analysis methods computationally [23], [24], [25], [26]. These evidences made it to be implemented here as the most suitable computational model. In short, this contribution emphasizes on

quantification and interpretation of specific bonding and electronic interactions in the isolated $H_2O$ molecule and $H_3O^+$, $H_5O_2^+$, and $H_9O_4^+$ hydrated states of the protons through these two analysis methods. The structure of this paper is organized as follows: the computational details are outlined in section 2, the results and discussions are presented in section 3, and the conclusions are summarized in section 4.

## II. Computational Details

Prior to determine the numeral values of the partial atomic charges for each hydrated proton: $H_3O^+$, $H_5O_2^+$, and $H_9O_4^+$, and an $H_2O$ molecule, and their 3D total electron density surfaces, MOs surfaces and contour maps, the most stable electronic structures of them were computed theoretically by using computationally designed molecular models as their trial structures. They were carefully built in *GaussView*: the Gaussian graphical interface [27], and the respective Cartesian coordinates of the atoms were extracted for geometry optimization. The concerned *Gaussian* keywords and methodologies were selected as instructed in *Gaussian* 09 manual [28]. The hybrid functional based DFT method known as B3LYP was employed with the basis set of this type: 6−31G (*d*, *p*) *i.e.*, the methodology applied was DFT: B3LYP/6−31G (*d*, *p*). To enforce *Gaussian* for carrying out desirable computations, ionic charge and spin multiplicity were specified as two integers in the format of (charge, spin multiplicity). Here, all the three hydrated protons are cationic with similar positive charge units, *i.e.*, $H_3O^+$, $H_5O_2^+$, and $H_9O_4^+$ have charge units of +1 each, and that for the $H_2O$ molecule is 0. Thus, the set of integers used in the *Gaussian* input file to describe former cationic forms and the latter neutral form were (1, 2), and (0, 1) respectively. Moreover, while solving the electronic Schrodinger equation iteratively, the self-consistent field (hereafter, SCF) with both default SCF procedure (SCF=Tight) and Berny algorithm for geometry optimizations to a local minimum were selected in *Gaussian* 09 [28], [29]. Since the current interest of this author is to study electronic and bonding interactions in the three most stable hydrated protons: $H_3O^+$, $H_5O_2^+$, and $H_9O_4^+$ ($H_2O$ molecule is taken here as a reference) through (a) MOs analysis: the 3D total electron density and MOs surfaces plus contours for each MO of these ionic and molecular specimens were constructed separately, and (b) Mulliken population analysis: all the concerned partial atomic charges of each specimen were displayed on the respective DFT derived ground state electronic structure on the basis of their color indices and ranges plus the respective numeral values of the atomic charges were also extracted, the *Gaussian* output files (such as *.log*, and *.fchk*) for each of them containing three dimensionally displayed chemical data were read by using *GaussView*, and sketched all the density surfaces/contours in the 3D plot axis.

## III. Results and Discussions

### 3.1 Bonding analysis

Every chemist accepts that the chemical bond and its in-depth analysis is a useful technique for acquiring semiquantitative type information applicable to explore the structural stability of the molecular/ionic specimens in their ground states. The two existing predominant electronic theories of chemical bonding: Lewis and VSEPR theory considered the bonding and non-bonding electron pairs as their central key-point, but both of them failed to clarify the critical role of the electron pairs such as distribution of bonding electrons in terms of orbitals (orbital concept), however, quantum mechanical theory had already started describing the electronic distributions in atoms more critically through the wave functions thinking about the electronic probabilistic matter waves [30], [31]. Therefore, an extensive examination of the proper behavior of the bonding and non-bonding electrons present in the molecular and ionic specimens may provide the fundamental roots for illuminating the theoretical insights into the chemical bonds. More specifically, a complete solution of the Schrödinger wave mechanical equation that describes the electronic wavefunction of the molecular or ionic systems may generate quantitative perspectives of the electronic interactions and chemical bonding [32], [33]. Unfortunately, it is not obvious to extract all the information related to the chemical bond from the molecular wavefunction due to the immeasurable and rigidly undefined concept of the bonding interactions [34]. Therefore, there are a number of ways of analyzing a theoretical calculation for the effective quantification of the electronic and bonding interactions in the ionic or nonionic molecular systems. These generally fall into several groups: (a) Molecular orbital analysis, (b) Population analysis, (c) Electron density analysis, and (d) Energy analysis. Being the nature of the chemical bonding a very complex and not rigorous type electronic interactions, none of these methods can fully capture the existence and characteristic features of the bonds and can provide even a little quantitative content on the bond lengths, bond angles, and strength of the bonds. However, these bond analysis techniques do have different types of skills to extract the reliable information about the bonding and electronic interactions from the molecular wavefunction, and therefore are already found to be indispensable tools to depict and quantify the specific type bonding interactions theoretically

[32], [33], [34]. In the present contribution, only first two methods, *viz.* Molecular orbital, and Population analysis are employed to analyze the DFT based theoretical calculations performed on the isolated $H_2O$ molecule, and $H_3O^+$, $H_5O_2^+$, and $H_9O_4^+$ states of the proton, and explored their bonding and electronic interactions separately. The detailed outcomes of these methods are summarized below in the subsections 3.1.1 and 3.1.2 respectively.

### 3.1.1 Molecular orbitals (MOs) analysis

According to MO theory, all the atomic orbitals ($\Psi_i$) of the atoms participating in the formation of the molecule approach nearer to each other and get mixed up to give an equivalent number of new orbitals called MOs ($\Psi$) [35]. On the basis of same principle, the MO energy level diagrams for the multi-atomic molecular/ionic systems can be constructed easily through which chemical bonding in them can be described qualitatively. However, this sort of diagrams for the MOs are only "cartoons" that can simply simplify a picture of the chemical bonding which is, however, a complex type electronic interactions. Fortunately, all the MOs that are involved to make up the concerned MO diagrams can be computed either in the form of a single total molecular electron density surface or in their separate single sets quantum mechanically. Figure 1 ((a) to (d)) displays the 3D total molecular electron density surfaces for the isolated $H_2O$ molecule, and $H_3O^+$, $H_5O_2^+$, and $H_9O_4^+$ states of the proton respectively. Each surface of each specimen is as a result of a complete association of the electron density of all the individual MOs of the same species. These total electron density surfaces represent electron density in the 3D space around the nuclei of the respective molecules/ions along with depicting probability of finding electrons around them in the 3D space. Mostly, these 3D electron density surfaces provide the geometrical patterns and a closed 3D molecular geometry plus symmetric and asymmetric distributions of the electron density around the specific atoms of such ionic species more precisely. In particular, the clearly distinguishable protrusions (electron dense regions) appeared at the electron density surface of each specimen speculate the orientations of the centrally bound chemical bonds in the 3D space. But, these total electron density surfaces do not give details about the specific arrangement of electron density in the particular type bond formation process. For it, the 3D electron density surface for each set of the MO of each molecular/ionic specimen must be sketched separately and observed individually on the basis of which atom-centered and localized or delocalized sites of the electron density as well as its significant probability of finding in the atomic proximity can be traced out easily. This sort of information eventually gives us a quantitative picture for elucidating the chemical bonding and electronic interactions that take place in between two similar or dissimilar bonding atoms in the molecules/ions. Again, for a further examination of the specific type bonding interactions, the contour plot for each MO must be used as it simply represents a slice through the molecule/ion along the plane joining specific atoms. Figure 2 ((a)−(d)), Figure 3((a)−(d)), Figure 4 ((a)−(h)), and Figure 5 ((a)−(p)) show the electron density surfaces and contour lines for each set of the real bonding MOs (containing two electrons with opposite spin) of the $H_2O$ molecule, and $H_3O^+$, $H_5O_2^+$, and $H_9O_4^+$ states of the proton respectively (core and nonbonding MOs are excluded). The captions include DFT derived Eigen value ($E$) for each MO in atomic unit (*a. u.*, Hartree $E_h$), and the concerned iso-surface value separately. Unfortunately, the atomic orbitals mixing coefficients (while constructing the MOs) are not computed here as the present computations were not aimed to perform Natural Bond Order (NBO) analysis. The careful analyses of these different sets of the MOs of these specimens make us to know that their electron densities are delocalized over the entire molecule/ions (the symmetry property of the MO) unlike the VBT assumptions which uses hybrid orbitals assigned to one specific atom and views the chemical bonds as localized electron pairs. Similarly, such delocalized type electron density surface for each MO of each molecular/ionic specimen not only describes the uniform/non-uniform distribution of the electrons over the entire molecule/ion, approximates a region of space in which valence electrons in the molecule/ions are likely to be found (spatial distribution of the electrons) but also assures us that each and every concerned MO is formed as a result of the orbital interactions of two or more than two atomic orbitals. Nevertheless, such MOs descriptions have set out the complete image of the molecular structure for each particular molecular/ionic specimen in which electrons are not assigned to individual bonds exist in between two similar or dissimilar atoms, but are treated as a cloud delocalized in the whole specimen. Moreover, the contour lines of each contour map of each MO of each specimen (Figure 2−Figure 5) that show electron amplitudes measuring a maximum departure of the electronic wave from its average value are also found to be extended over the whole molecular/ionic specimen. Thus, the contour maps and the electron density surface plots of the MOs confirm the bonding and structural entities of all the three stable hydrated states of the proton quantum mechanically. In short, the structural stabilities, molecular/ionic entities, and the electronic interactions & chemical bonding of the $H_2O$ molecule, and $H_3O^+$, $H_5O_2^+$, and

$H_9O_4^+$ states are visualized and explained quantitatively through the MOs analysis method.

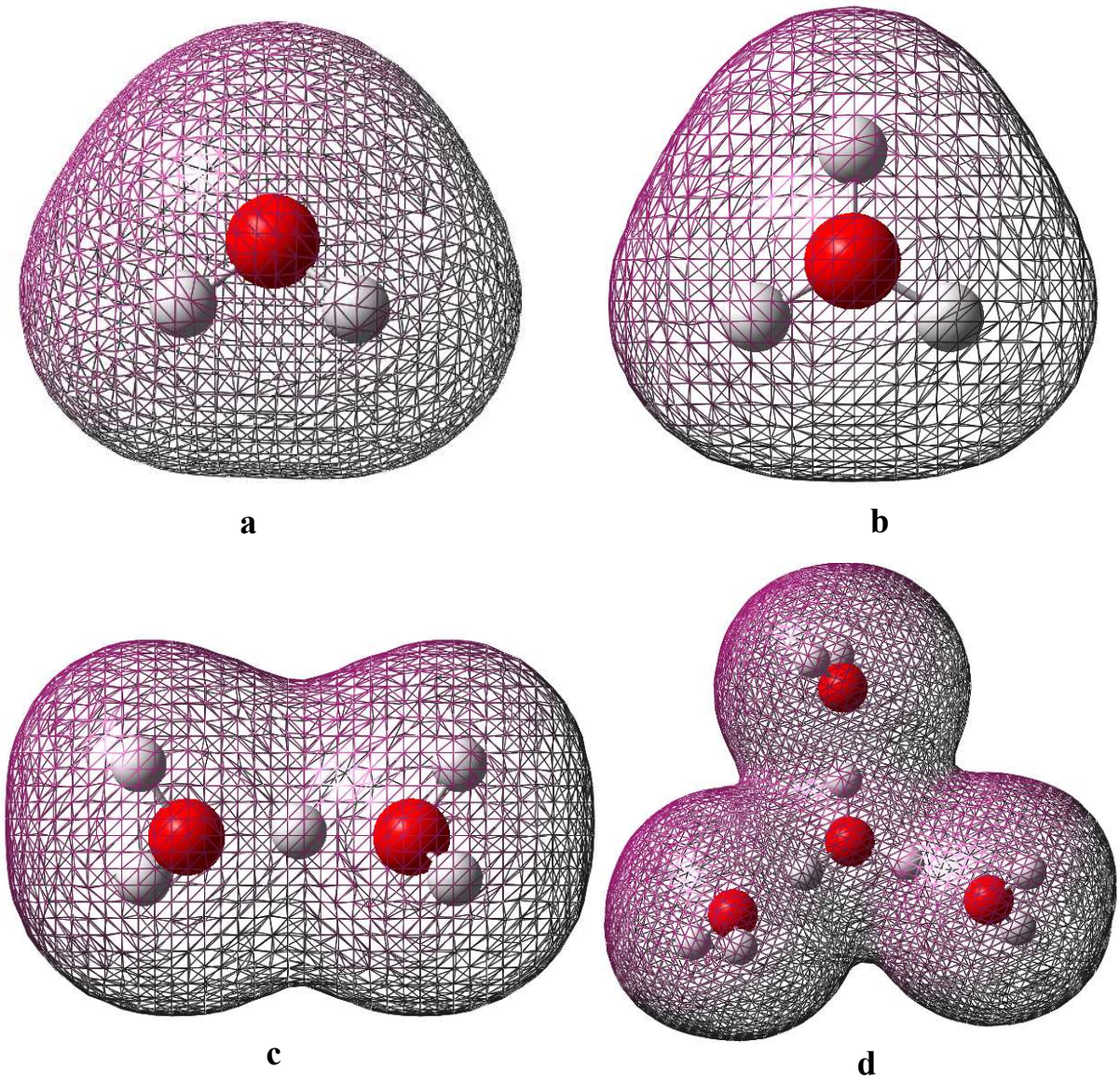


Figure 1. Total electron density surface for an (a) $H_2O$ molecule, (b) $H_3O^+$ ion, (c) $H_5O_2^+$ ion, and (d) $H_9O_4^+$ ion at |isovalue|: MO = 0.0200, and Density = 0.0004. The individual MOs that make up each of these density surfaces are shown in Figure 2 to Figure 5 respectively.

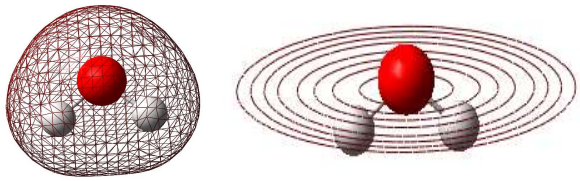

**(a) 2a MO and contours, $E = -0.99735$ *a.u***

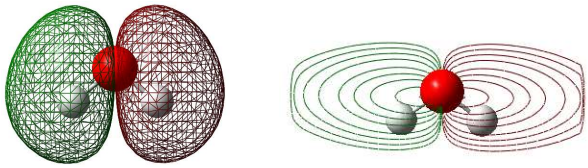

**(b) 3a MO and contours, $E = -0.51502$ *a.u.***

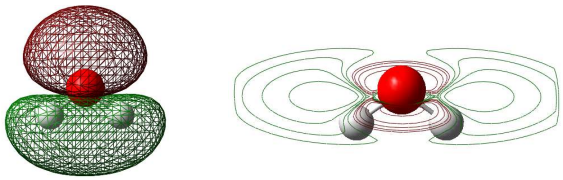

**(c) 4a MO and contours, $E = -0.37102$ *a.u.***

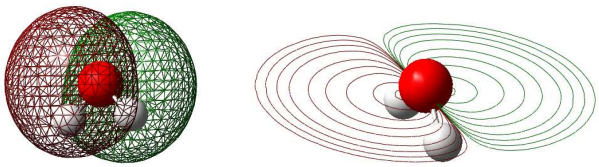

**(d) 5a MO and contours, $E = -0.29197$ *a.u.***

Figure 2. DFT computed real MOs of an $H_2O$ at isovalue = 0.02. They collectively make up the total electron density surface of it displayed in Figure 1(a). The core MOs are excluded.

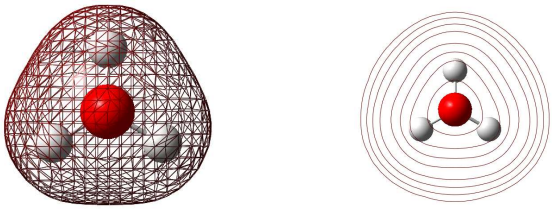

**(a) 2a MO and contours, $E = -1.45037$ *a.u.***

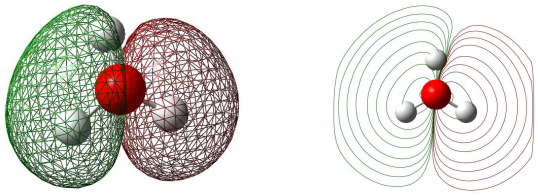

**(b) 3a MO and contours, $E = -0.93882$ *a.u.***

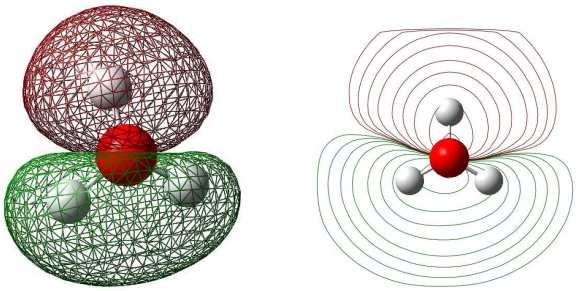

**(c) 4a MO and contours, $E = -0.93882$ *a.u.***

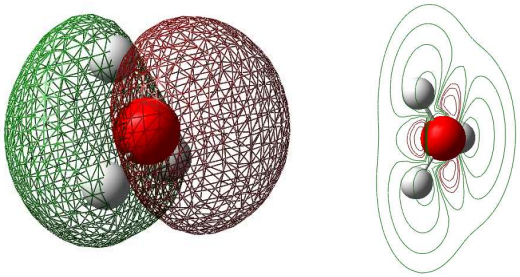

**(d) 5a MO and contours, $E = -0.73832$ *a.u.***

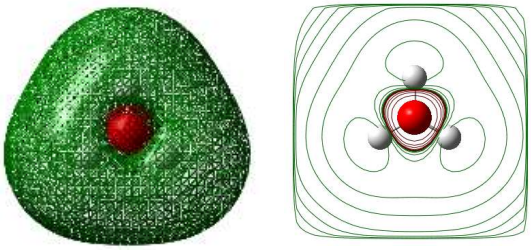

**(e) 6a MO and contours, $E = -0.26456$ *a.u.***

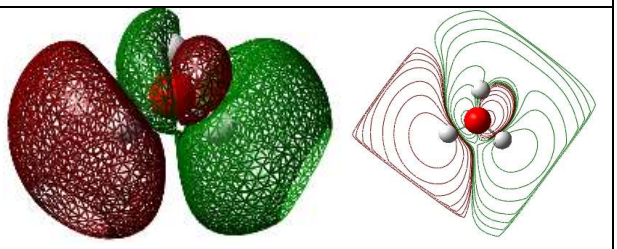

**(f) 7a MO and contours, $E = -0.16215$ *a.u.***

Figure 3. DFT computed real MOs of an $H_3O^+$ ion at isovalue = 0.02. They collectively make up the total electron density surface of it displayed in Figure 1(b). The core MOs are excluded.

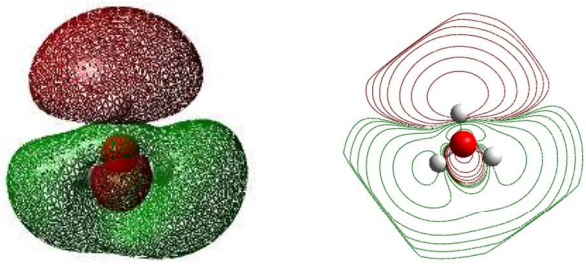

**(g) 8a MO and contours, *E* = − 0.16215 *a.u*.**

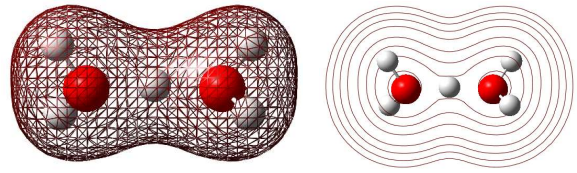

**(a) 3a MO and contours, *E* = − 1.31969 *a.u.***

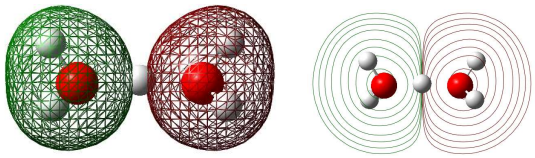

**(b) 4a MO and contours, *E* = − 1.29198 *a.u***

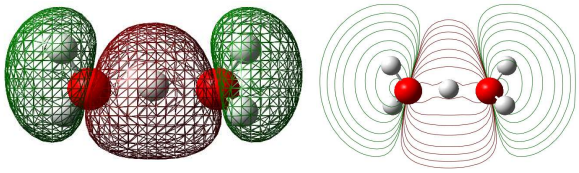

**(c) 5a MO and contours, *E* = − 0.83626 *a.u***

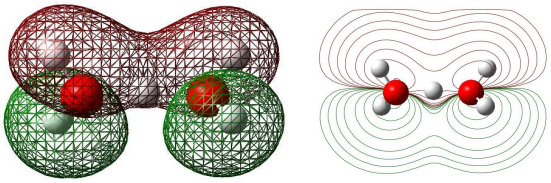

**(d) 6a MO and contours, *E* = − 0.81688 *a.u.***

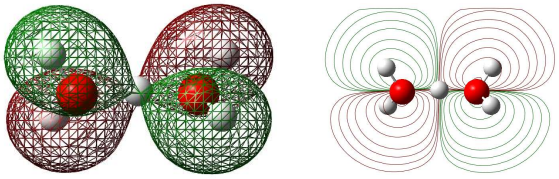

**(e) 7a MO and contours, *E* = − 0.81599 *a.u.***

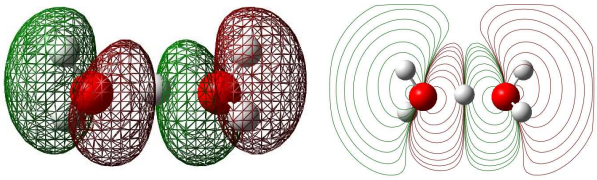

**(f) 8a MO and contours, *E* = − 0.67216 *a.u.***

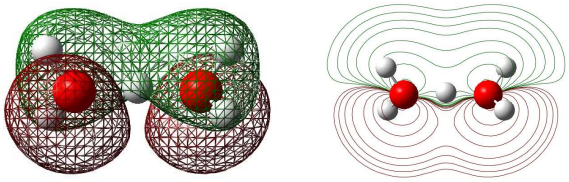

**(g) 9a MO and contours, *E* = − 0.60751 *a.u.***

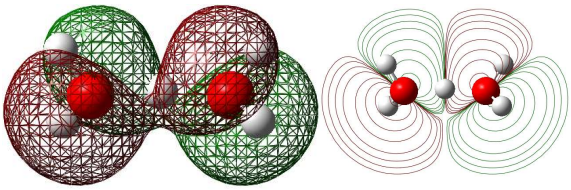

**(h) 10a MO and contours, *E* = − 0.59836 *a.u.***

Figure 4. DFT computed real MOs of an $H_5O_2^+$ ion at isovalue = 0.02. They collectively make up the total electron density surface of it displayed in Figure 1(c). The core MOs are excluded.

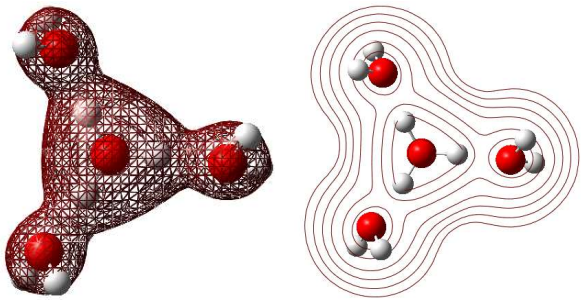

(a) 5a MO and contours, $E = -1.08623$ *a.u.*

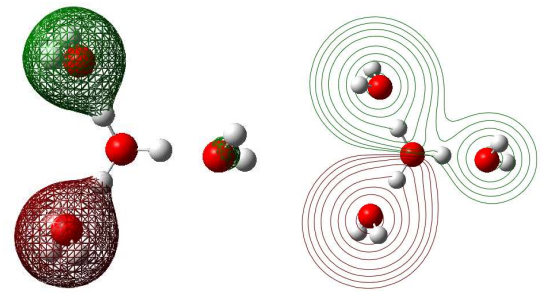

(b) 6a MO and contours, $E = -1.03876$ *a.u.*

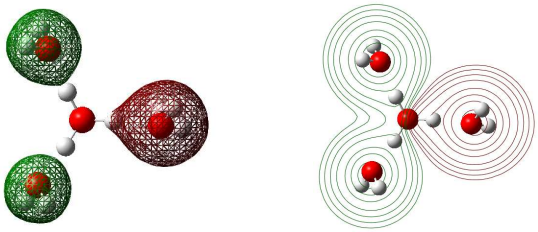

(c) 7a MO and contours, $E = -1.03872$ *a.u.*

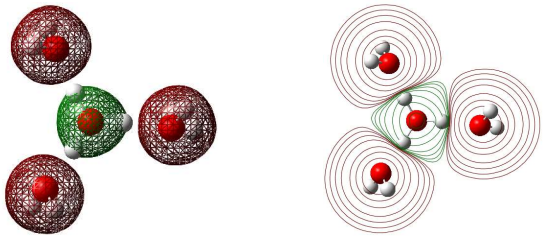

(d) 8a MO and contours, $E = -1.03204$ *a.u.*

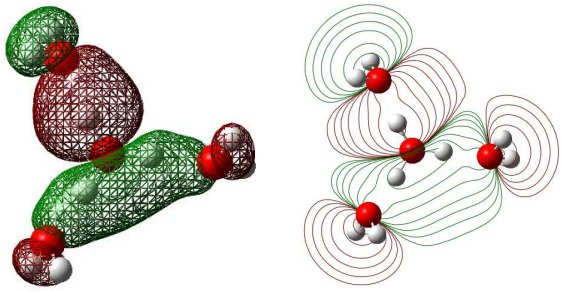

(e) 9a MO and contours, $E = -0.59560$ *a.u.*

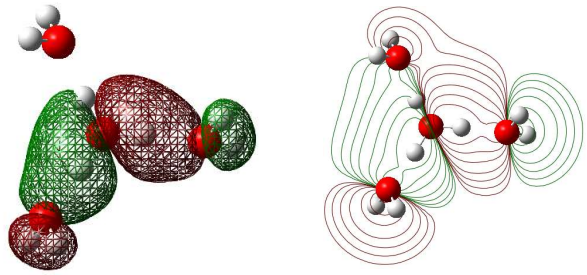

(f) 10a MO and contours, $E = -0.59555$ *a.u.*

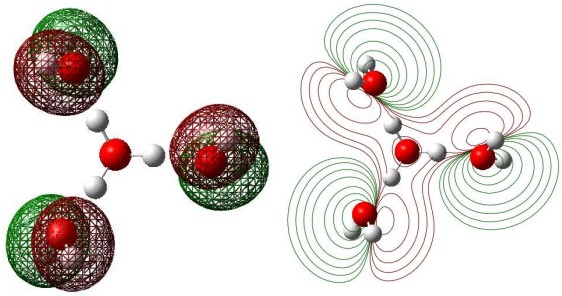

(g) 11a MO and contours, $E = -0.55297$ *a.u.*

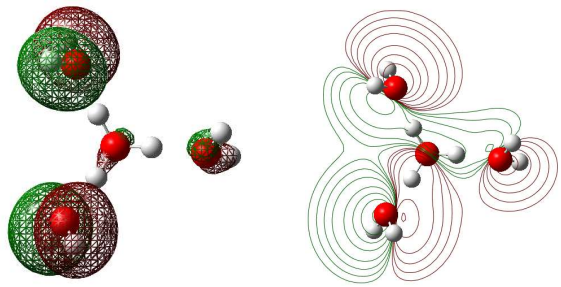

(h) 12a MO and contours, $E = -0.55297$ *a.u.*

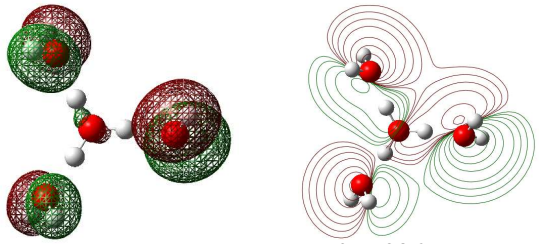

(i) 13a MO and contours, $E = -0.55236$ *a.u.*

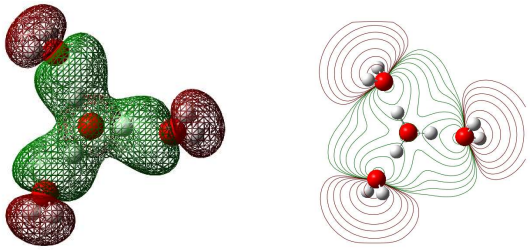

(j) 14a MO and contours, $E = -0.45488$ *a.u.*

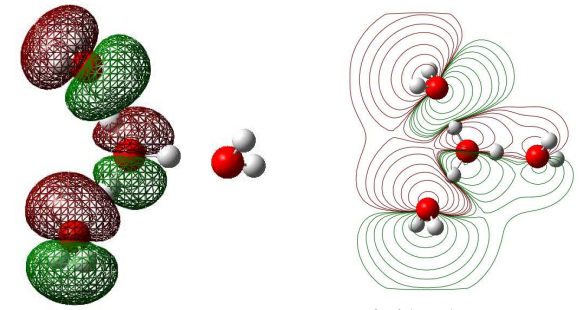

**(k) 15a MO and contours, $E = -0.41551$ *a.u.***

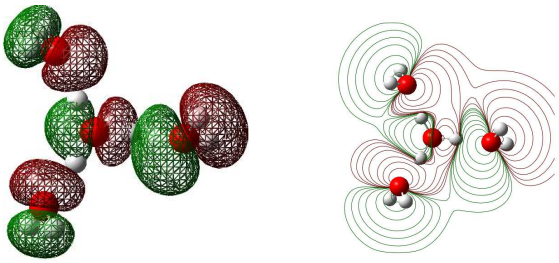

**(l) 16a MO and contours, $E = -0.41547$ *a.u.***

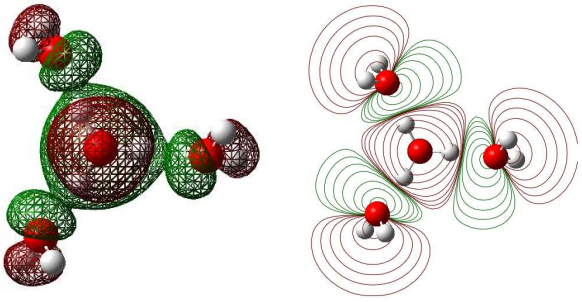

**(m)17a MO and contours, $E = -0.38938$ *a.u.***

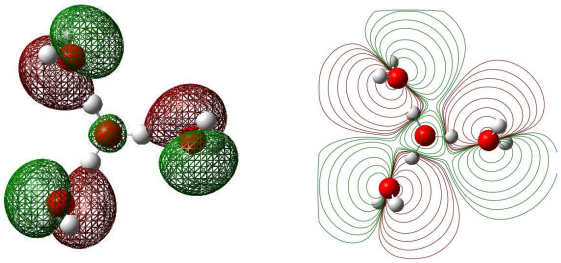

**(n) 18a MO and contours, $E = -0.35144$ *a.u.***

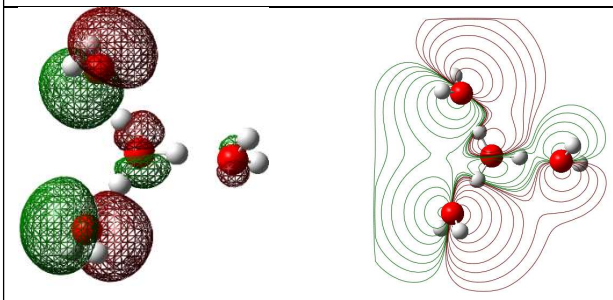

**(o) 19a MO and contours, $E = -0.34774$ *a.u.***

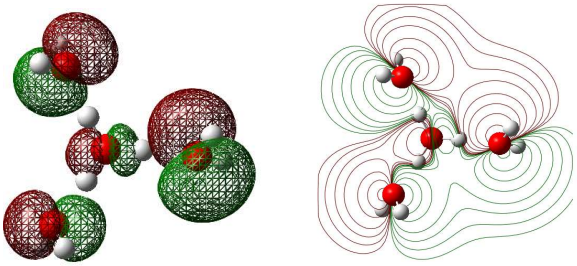

**(p) 20a MO and contours, $E = -0.34769$ *a.u.***

Figure 5. DFT computed real MOs of an $H_9O_4^+$ ion at isovalue = 0.02. They collectively make up the total electron density surface of it displayed in Figure 1(d). The core MOs are excluded.

### 3.1.2 Mulliken population analysis

The above explained MOs representation through the electron density mapping techniques are quite informative to understand the chemical bonding and electronic interactions deeply, however we often need the numerical values of the atomic charges to quantify and compare specific type atomic interactions. As a rule, assigning partial charges on each atom is very much important in order to get a qualitative idea of the charge distribution in the molecular/ionic specimens. Theoretically, the population analysis methods that divide up the $D_{\alpha\beta}S_{\alpha\beta}$ term of the orbital occupation $\rho(r)$ expression ($\because \rho(r) = D_{\alpha\beta}S_{\alpha\beta}$; density and overlap matrix terms respectively) can derive the numeral values of atomic charges that tell us approximately about where the electron density actually resides in the molecular/ionic systems [15]. Though it is not recommended to over interpret the data of the partial atomic charges provided by any of the population analysis methods as they do not represent an observable property of atoms or molecules, the partial atomic charge on each atom derived through the most common and widely used Mulliken population analysis method is very useful to understand the charge distribution in the systems qualitatively. Technically, the Mulliken analysis operates by summing up all the populations for all the atomic orbitals on a single atom, and then subtracting the nuclear charge to give the resultant partial atomic charge on each atom [15], [16]. The DFT

derived Mulliken atomic charges distribution in the hydrogen, and oxygen atoms of the $H_2O$ molecule, and hydrated protons: $H_3O^+$, $H_5O_2^+$, and $H_9O_2^+$ are presented in Table 1, where all the numerically labeled atoms are listed in accordance with the atomic label presented in Figure 6(a−d) respectively. On the basis of an intensity of Mulliken atomic charges, all the atoms of the molecular and ionic specimens are colored and displayed as their DFT derived ground state electronic structures (Figure 6), where color indices and ranges are clearly mentioned. From the color indices of each of these optimized structures, it can be concluded that all the red colored (in $H_2O$: O1; in $H_3O^+$: O1; in $H_5O_2^+$: O1 and O4; in $H_9O_4^+$: O1, O5, O8, and O11), the most green colored (in $H_3O^+$: H2, H3 and H4; in $H_5O_2^+$: H2, H3, H5, H6, and H7; in $H_9O_4^+$: H2, H3, H4), and the dark green colored (in $H_3O^+$: H2, and H3; in $H_9O_4^+$: H6, H7, H9, H10, H12, H13) spheroids represent the most negatively, most positively, and less positively charged atoms respectively. The same observation can be reconfirmed by analyzing the concerned numeral Mulliken atomic charges listed in Table 1. More importantly, the H5 atom in $H_5O_2^+$ ion is comparatively more positively charged due to its involvement in hydrogen bond (hereafter, H−bond) with more electronegative O1 and O4 atoms that hold directly bonded H2, H3 and H6, H7 atoms respectively. Similarly, as the central $H_3O$ unit of the $H_9O_4^+$ is linked with three electronegative O5, O8, and O11 atoms of the three nearby $H_2O$ molecules by three different H−bonds, it is obvious to become H2, H3, and H4 atoms more positively charged as can be seen in Table 1, even more positive than the H−bond free H2, H3, and H4 atoms of the $H_3O^+$ ion. As a whole, such inhomogeneous charge distributions in either of these molecular/ionic specimens are mostly arose due to a strong ability of the O atom to attract a bond pair towards itself as its electronegativity ($\chi_O$ = 3.44 in Pauling scale) is significantly greater than that of the H ($\chi_H$ = 2.20 in Pauling scale) atom. This effect is more pronounced in the H−bonded oxygen and hydrogen atoms as observed in $H_5O_2^+$ and $H_9O_4^+$ states.

Since an absolute magnitude of the atomic charges computed by the Mulliken population analysis method displays a high degree of sensitivity to the types of basis set used, and therefore is subjected to vary with respect to latter, the above presented numeral values were only restricted to the basis set of the type 6−31G (*d, p*). Because of this reason, an over interpretation of the Mulliken derived partial atomic charges is not recommended.

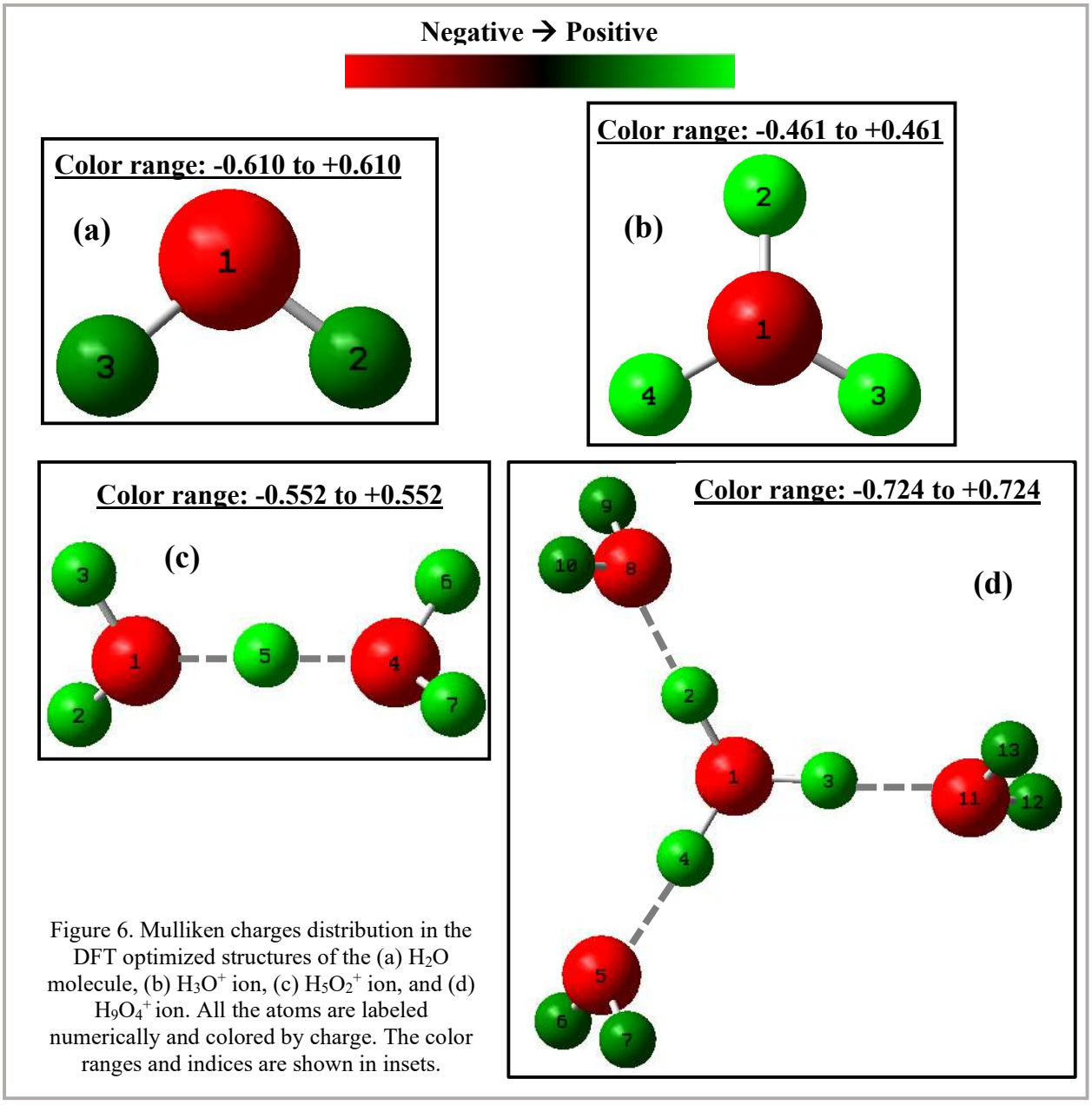


Figure 6. Mulliken charges distribution in the DFT optimized structures of the (a) $H_2O$ molecule, (b) $H_3O^+$ ion, (c) $H_5O_2^+$ ion, and (d) $H_9O_4^+$ ion. All the atoms are labeled numerically and colored by charge. The color ranges and indices are shown in insets.

Table 1. Mulliken charges distribution in an (a) $H_2O$ molecule, (b) $H_3O^+$ ion, (c) $H_5O_2^+$ ion, and (d) $H_9O_4^+$ ion

**(a)**

| S. No. | Atoms | Mulliken charge (*a. u.*) |
|---|---|---|
| 1 | O1 | −0.610 |
| 2 | H2 | + 0.305 |
| 3 | H3 | +0.305 |
| Sum of the Mulliken atomic charges = 0.00 *a.u.* | | |

**(b)**

| S. No. | Atoms | Mulliken charge (*a. u.*) |
|---|---|---|
| 1 | O1 | −0.382 |
| 2 | H2 | + 0.461 |
| 3 | H3 | +0.461 |
| 4 | H4 | +0.461 |
| Sum of the Mulliken atomic charges = 1.00 *a.u.* | | |

**(d)**

| S. No. | Atoms | Mulliken charge (*a. u.*) |
|---|---|---|
| 1 | O1 | −0.724 |
| 2 | H2 | + 0.536 |
| 3 | H3 | +0.536 |
| 4 | H4 | +0.536 |
| 5 | O5 | −0.681 |
| 6 | H6 | +0.359 |
| 7 | H7 | +0.361 |
| 8 | O8 | −0.681 |
| 9 | H9 | +0.358 |
| 10 | H10 | +0.361 |
| 11 | O11 | −0.681 |
| 12 | H12 | +0.358 |
| 13 | H13 | +0.361 |
| Sum of the Mulliken atomic charges = 0.999 *a.u.* | | |

**(c)**

| S. No. | Atoms | Mulliken charge (*a. u.*) |
|---|---|---|
| 1 | O1 | −0.552 |
| 2 | H2 | + 0.405 |
| 3 | H3 | +0.403 |
| 4 | O4 | −0.552 |
| 5 | H5 | +0.490 |
| 6 | H6 | +0.403 |
| 7 | H7 | +0.405 |
| Sum of the Mulliken atomic charges = 1.00 *a.u.* | | |

## IV. Conclusion

This study gave theoretical insights into the chemical bonding in Hydronium ($H_3O^+$), Zundel ($H_5O_2^+$), and Eigen ($H_9O_4^+$) states of proton from the analysis of their molecular wave functions through molecular orbitals (MOs) and Mulliken population analysis methods. Basically, these methods were applied here to analyze the DFT based quantum mechanical calculations performed on these three micro-hydrated states of the protons. The unanimous choice of the DFT model was due to its extraordinary skills to incorporate even a minimal but significant strength of the micro-particles interactions ($H^+$ and $H_2O$ interact during proton hydration process) substantially without which accurate determination of the ground state electronic structures and reliable 3D electron density surfaces of the molecular orbitals plus absolute magnitudes of the partial atomic charges for these three hydrated states couldn't have been obtained computationally.

More precisely, the MOs and population analysis methods were used to extract chemical bond related information from the molecular wavefunction ($\Psi$) and then a quantitative picture for the $\Psi$ was directly inquired by looking into total molecular electron density ($\Psi^2$) surfaces followed by the careful examination of the iso-surfaces and contours of each MO. The general results show that the total molecular electron density surface for each hydrated state represented a

closed 3D molecular geometry plus symmetric and asymmetric distributions of the electron cloud around the specific atoms precisely. Apart from this, the clearly distinguishable protrusions appeared at each density surface of each state speculated the orientations of centrally bound chemical bonds in the 3D space. Similarly, the close analyses of different sets of the MOs of each hydrated state indicated the complete delocalization of their electron density surfaces over the entire molecular species which not only approximated a region of space in which valence electrons are likely to be found but also assured that each MO is formed as a result of the orbital interactions of two similar or dissimilar atomic orbitals. Moreover, the contour lines for each contour map of each MO were found to be expanded over the whole ionic specimen and exhibited the electron amplitudes clearly. As a whole, both the electron density surface plots and the contour maps confirmed the bonding and structural entities of all the three stable hydrated states of the protons quantum mechanically. Additionally, the Mulliken derived partial atomic charge on each atom of these hydrated protons gave insights into the charge distribution in them qualitatively that was indeed quite useful while quantifying and comparing specific bonding interactions.

Even though the MOs and the Mulliken population analysis methods were applied here to give quantum mechanical views of the chemical bonds and electronic interactions in the Hydronium ($H_3O^+$), Zundel ($H_5O_2^+$), and Eigen ($H_9O_4^+$) states of the proton and to reveal quantitative pictures of their bonding interactions and structural entities theoretically, one may perform natural bond order (NBO) type calculations for getting comparatively better picture of the electron density distributions in atoms and in bonds between the atoms. It is suggested to compute atomic orbitals mixing coefficients for each MO of these cations so that one can easily predict the quantum superposition of their atomic orbitals through LCAO approach.

**REFERENCES**


[1] C. J. D. von Grotthuss, Ann. Chim. LVIII, 54(1806).

[2] J. M. Headrick, E. G. Diken, R. S. Walters, N. I. Hammer, R. A. Christie, J. Cui, E. M. Myshakin, M. A. Duncan, M. A. Johnson, K. D. Jordan, Science 308, 1765(2005).

[3] K. R. Asmis, N. L. Pivonka, G. Santambrogio, M. Brummer, C. Kaposta, D. M. Neumark, L. Wo¨ste, Science 299, 1375(2003). (b) M. Miyazaki, A. Fujii, T. Ebata, N. Mikami Science 304, 1134(2004). (c) J. W. Shin, N. I. Hammer, E. G. Diken, M. A. Johnson, R. S. Walters, T. D. Jaeger, M. A. Duncan, R. A. Christle, K. D. Jordan, Science 304, 1137(2004). (d) C. C. Wu, C. K. Lin, H. C. Chang, J. C. Jiang, J. L. Kuo, M. L. Klein, J. Chem. Phys.122, 074315(2005).

[4] A.B. Marahatta, Int. J. Prog. Sc. Tech. 22(2), 290(2020).

[5] A.B. Marahatta, Int. J. Prog. Sc. Tech. 23(1), 473(2020).

[6] N. Agmon, Chem. Phy. Lett. 244(5–6), 456(1995).

[7] J. Han, H. Liu, Proceedings of IMECE2005, IMECE2005–81340, 1(2005).

[8] Y. S. Park, T. Hatae, H. Itoh, M. Y. Jang, Y. Yamazaki, Electrochimica Acta, 50(2–3), 592(2004).

[9] S. Banerjee, D. E. Curtin, J. Fluorine Chem. 125(8), 1211(2004).

[10] A.B. Marahatta, Int. J. Prog. Sc. Tech. 17(1), 55(2019).

[11] A.B. Marahatta, Int. J. Prog. Sc. Tech. 18(2), 43(2020).

[12] A.B. Marahatta, Int. J. Prog. Sc. Tech. 22(1), 67(2020).

[13] A.B. Marahatta, Int. J. Prog. Sc. Tech. 19(1), 100(2020).

[14] P. Hunt, B. Kirchner and T. Welton, Chem. Eur. J. 12(26), 6762(2006).

[15] F. Jensen, Introduction to Computational Chemistry (John Wiley & Sons, Chichester, 2003).

[16] W. L. Jolly, Modern Inorganic Chemistry (McGraw-Hill Book Company, New York, 1984).

[17] K. Fukui, Science 218(4574), 747(1982).

[18] J. B. Foresman, Æ Frisch, Exploring Chemistry with Electronic Structure Methods (Gaussian, Inc.: Wallingford, CT, 2015).

[19] R. S. Mulliken, J. Chem. Phys. 23, 1833(1955).

[20] M. D. Segall, R. Shah, C. J. Pickard, M. C. Payne, Phys. Rev. B 54(23), 16317(1996).

[21] P. Hohenberg, W. Kohn, Phys. Rev. B 136(3B), 864(1964).

[22] W. Kohn, L. Sham, Phys. Rev. J. 140(4A), A1133 (1965).

[23] A.B. Marahatta, Int. J. Prog. Sc. Tech. 16(1), 51(2019).

[24] A.B. Marahatta, Int. J. Prog. Sc. Tech. 16(2), 01(2019).

[25] Wang, S. L. Li, D. G. Truhlar, J. Chem. Theory Comput. 10, 5640(2014).

[26] R. Z. Khaliullin, A. T. Bell, M. Head-Gordon, J. Chem. Phys. 128, 184112-1(2008).

[27] Æ. Frisch, H. P. Hratchian, R. D. Dennington II, T. A. Keith, J. Millam, Gauss view 05 Reference (Gaussian, Inc.: Wallingford, CT, 2009).

[28] Gaussian 09 manual. http://gaussian.com/geom/?tabid=1#GeomkeywordReadOptimi zeoption

[29] Æ. Frisch, Gaussian 09W Reference (Gaussian, Inc.: Wallingford, CT, 2009).

[30] J. Rigby, E. I. Izgorodina, Phys. Chem. Chem. Phys. 15, 1632(2013).

[31] G. V. Gibbs, A. F. Wallace, D. F. Cox, R. Downs, N. L. Ross, K. M. Rosso, Am. Mineral. 94, 1085(2009).

[32] L. Pauling, J. Chem. Educ. 69, 519(1992).

[33] G. Frenking, A. Krapp, J. Comput. Chem. 28, 15(2007).

[34] M. Fugel, J. Beckmann, D. Jayatilaka, G. V. Gibbs, S. Grabowsky, Chem. Eur. J. 24, 6248(2018).

[35] R. D. Madan, Modern Inorganic Chemistry (S. Chand & Company: India, 1997).